Vol 14 No 3, March 2005
1009-1963/2005/14(03)/0620-08

Chinese Physics

© 2005 Chin. Phys. Soc.
and IOP Publishing Ltd

Eulerian simulation of sedimentation flows in vertical and inclined vessels*

Wu Chun-Liang(吴春亮) and Zhan Jie-Min(詹杰民)†

Department of Applied Mechanics and Engineering, Zhongshan University, Guanzhou 510275, China

(Received 5 August 2004; revised manuscript received 4 November 2004)

Sedimentation of particles in inclined and vertical vessels is numerically simulated using a finite volume method where the Eulerian multiphase model is applied. The particulate phase as well as the fluid phase is regarded as a continuum while the viscosity and solid stress of the particulate phase are modelled by the kinetic theory of granular flows. The numerical results show an interesting phenomenon of the emergence of two circulation vortices of the sedimentation flow in a vertical vessel but only one in the inclined vessel. Several sensitivity tests are simulated to understand the factors that influence the dual-vortex flow structure in vertical sedimentation. Results show that a larger fluid viscosity makes the two vortex centres much closer to each other and the boundary layer effect at lateral walls is the key factor to induce this phenomenon. In the fluid boundary layer particles settle down more rapidly and drag the local carrier fluid to flow downward near the lateral walls and thus form the dual-vortex flow pattern.

Keywords: sedimentation of particles, vortices, Eulerian simulation
PACC: 7970

1. Introduction

The removal of solid particles from liquid or gas streams by means of gravity is an important step in many industrial processes and environment control systems. A number of theoretical and numerical studies have given insight into the particle separation from suspended mixture in a container since Boycott[1] reported that by tilting the container corpuscles separate from blood a good deal faster than in a vertical container and their results gave good agreement with experiment. Richardson and Zaki[2] gave the empirical expression of the settling velocity of a monodisperse suspension. Batchelor[3] derived the dilute suspension limit for the sedimentation velocity. De Kruif *et al*[4] gave an experimental result of sedimentation velocity for silica spheres.

More researches focus on the "Boycott effect". Ponder[5] and Nakamura and Kuroda[6] presented independently a quantitative prediction known as the PNK theory for the sedimentation rate of inclined settling process between parallel plates based on a kinematics model. Kinosita[7] observed in experiments that there exists a rapid convective vortex pattern within the main body of the suspension and measured the particle velocities as high as 100 times the Stokes velocity. Hill *et al*[8] studied this phenomenon theoretically using the appropriate equations of continuum mechanics but limited their investigation to very dilute suspensions and negligibly small particle Reynolds numbers. Acrivos and Herbolzheimer[9] extended Hill *et al*'s work for arbitrary particle initial concentration and geometry of the settling vessel and presented a modified PNK theory which give good predictions of sedimentation rate in their experiments for different angels of inclination. Herbolzheimer[10] observed instabilities at the upper clarified liquid interface and investigated the conditions of wave formation and growth using a linear stability theory. By solving the modified Rayleigh equation Zhou and Lin[11] studied the instability of inviscid mixing layer considering the effect of suspended particles. Lin and Nie reported that the cylindrical particles have a suppression effect on the flow instability at a two-phase boundary layer.[12]

Numerical simulation has become a very important tool to study some complex particulate flows and

*Project supported by the National Natural Science Foundation of China (Grant No 40476012), and the Research Fund for the Doctoral Program of Ministry of Education of China (No 20020558013).

†E-mail: stszjm@zsu.edu.cn

the above experimental and theoretical sedimentation physics gives good verifications to numerical models and schemes. Rather than analytical or empirical methods, a numerical approach is more suitable for complex geometry and special conditions and numerical tests are more easily repeated than experiments. To date the difference between mathematical models of separated particulate multiphase flow which numerical schemes are based on lies in the different ways of modelling the particle phase, namely the Lagrangian approach and the Eulerian continuum model.

A famous Lagrangian method is the multiphase particle-in-cell (MP-PIC) method, which has been presented by Andrews and O'Rourke and Snider *et al*[13,14] for particulate flows that accounts for full coupling between the fluid and particle phase as well as the interparticle stress due to collisions. Unlike the discrete particle method[15–17] that calculates the collision forces or detects collisions between particles and then calculates particle movement after collision, the MP-PIC method computes the interparticle stress on Eulerian grids and then the stress gradients are calculated and mapped back to particle positions when computing the particle movements. The MP-PIC method has been applied to many applications such as bimodal sedimentation, sediment flow in inclined vessels, particulate flow of a reservoir fracture, and bubbling fluidized bed.[14,18] Recently the lattice Boltzmann method for fluid phase combined with the Lagrangian trajectory model for particles are developed and applied to simulations of movement of spherical particles in a three-dimensional domain[19] and particle-laden flow over a backward-facing step.[20]

In this paper we use an Eulerian two-fluid approach to simulate the sedimentation flows in vertical vessels and vessels having inclined walls. More attention is paid to the flow physical dynamics captured by the numerical simulations rather than to the numerical scheme itself. Though Eulerian multiphase model has been widely used in many numerical computations such as simulations of bubbling fluidized bed, circulating fluidized bed and bubble column reactors,[21–24] there has been no literature, to the authors' knowledge, using this method to simulate particulate flows of sedimentation. By the Eulerian approach the interparticle collision stress and the particle viscosity are modelled by the kinetic theory of granular flows. The numerical results first show the dual-circulation flow patterns of sedimentation in a vertical vessel, and that the fluid viscosity and wall boundary conditions have significant effect on this phenomenon.

2. Governing equations

In contrast to the Lagrangian approach, to trace individual particles in the Eulerian two-fluid model the particulate phase as well as the fluid phase is handled as a continuum. Thus the fluid and dispersed particle phases can be described mathematically in similar mass and momentum balances. We use the continuity and momentum equations for both phases presented by Ding and Gidaspow.[21]

2.1. Mass and momentum balances

The accumulation of mass in each phase is balanced by the convective mass fluxes without interphase mass transfer:

$$\frac{\partial}{\partial t}\left(\rho_i \varepsilon_i\right) + \nabla \cdot \left(\rho_i \varepsilon_i \boldsymbol{u}_i\right) = 0, \tag{1}$$

where ε_i is the volume fraction, ρ_i the density and $\boldsymbol{u}_i$ the average velocity (i denotes the liquids or solids).

In the sedimentation flow only drag forces between particles and liquid phase are taken into account with other forces such as virtual mass force, lift force and Basset force being negligible. The momentum equations of the two phases are given as follows:
liquids:

$$\begin{aligned}&\frac{\partial}{\partial t}\left(\rho_\mathrm{l}\varepsilon_\mathrm{l}\boldsymbol{u}_\mathrm{l}\right) + \nabla \cdot \left(\rho_\mathrm{l}\varepsilon_\mathrm{l}\boldsymbol{u}_\mathrm{l}\boldsymbol{u}_\mathrm{l}\right)\\ &= -\varepsilon_\mathrm{l}\nabla p + \nabla \cdot \bar{\bar{\boldsymbol{\tau}}}_\mathrm{l} + \rho_\mathrm{l}\varepsilon_\mathrm{l}\boldsymbol{g} - \beta\left(\boldsymbol{u}_\mathrm{l} - \boldsymbol{u}_\mathrm{s}\right),\end{aligned} \tag{2}$$

solids:

$$\begin{aligned}&\frac{\partial}{\partial t}\left(\rho_\mathrm{s}\varepsilon_\mathrm{s}\boldsymbol{u}_\mathrm{s}\right) + \nabla \cdot \left(\rho_\mathrm{s}\varepsilon_\mathrm{s}\boldsymbol{u}_\mathrm{s}\boldsymbol{u}_\mathrm{s}\right)\\ &= -\varepsilon_\mathrm{s}\nabla p - \nabla p_\mathrm{s} + \nabla \cdot \bar{\bar{\boldsymbol{\tau}}}_\mathrm{s} + \rho_\mathrm{s}\varepsilon_\mathrm{s}\boldsymbol{g} + \beta\left(\boldsymbol{u}_\mathrm{l} - \boldsymbol{u}_\mathrm{s}\right),\end{aligned} \tag{3}$$

with

$$\bar{\bar{\boldsymbol{\tau}}}_i = \varepsilon_i\mu_i\left(\nabla\boldsymbol{u}_i + \nabla\boldsymbol{u}_i^\mathrm{T}\right) + \varepsilon_i\left(\lambda_i - \frac{2}{3}\mu_i\right)\nabla \cdot \boldsymbol{u}\bar{\bar{\boldsymbol{I}}}, \tag{4}$$

where λ_i is the bulk viscosity which is set to zero for fluid phase and μ_i is the shear viscosity, p the static pressure with p_s the solid's pressure.

2.2. Interphase force

The interphase force represents the momentum coupling or exchange between two phases and is denoted by a drag term in the momentum equations. The drag coefficient used here is presented by Ding and Gidaspow.[21]

In a dilute region when $\varepsilon_l \geq 0.8$ a modified Stokes equation based on empirical correlation gives

$$\beta = \frac{3}{4} C_D \frac{\varepsilon_s \varepsilon_l \rho_l \left| \boldsymbol{u}_l - \boldsymbol{u}_s \right|}{d_s} \varepsilon_l^{-2.65}, \tag{5}$$

where

$$C_D = \frac{24}{\mathrm{Re}} \left(1 + 0.15 \mathrm{Re}^{0.687}\right), \tag{6}$$

and

$$\mathrm{Re} = \frac{\varepsilon_l \rho_l \left| \boldsymbol{u}_l - \boldsymbol{u}_s \right| d_s}{\mu_l}. \tag{7}$$

When $\varepsilon_l < 0.8$ where the sedimentation is nearly close packed the following equation for packed fluidized bed gives

$$\beta = 150 \frac{\varepsilon_s^2 \mu_l}{\varepsilon_l d_s^2} + 1.75 \frac{\rho_l \varepsilon_s \left| \boldsymbol{u}_l - \boldsymbol{u}_s \right|}{d_s}. \tag{8}$$

2.3. Kinetic model for the dispersed phase

We adopt the kinetic theory of granular flows to model the interactions between particles. The theory is based on the kinetic theory of dense gases[25] and was developed mainly by Savage and Jeffrey,[26] Jenkins and Savage,[27] and Lun *et al.*[28] Ding and Gidaspow[21] as well as Syamlal *et al*[23] applied the theory and implemented numerical models to fluidized bed simulations.

In the kinetic theory of granular flows a new property of the dispersed phase known as the granular temperature that represents the particle fluctuating energy is expressed as

$$\Theta = \frac{1}{3} \left\langle C_i C_i \right\rangle, \tag{9}$$

where C_i is the particulate phase fluctuation velocity (the brackets denote ensemble averaging).

According to Ding and Gidaspow[21] as well as Gidaspow,[22] the solid pressure can be calculated:

$$p_s = \varepsilon_s \rho_s \left[1 + 2\left(1 + e\right) \varepsilon_s g_0\right] \Theta. \tag{10}$$

The solid shear viscosity is

$$\mu_s = \frac{4}{5} \varepsilon_s \rho_s d_s g_0 \left(1 + e\right) \sqrt{\frac{\Theta}{\pi}} + \frac{10 \rho_s d_s \sqrt{\Theta \pi}}{96 \varepsilon_s \left(1 + e\right) g_0} \times \left[1 + \frac{4}{5} \varepsilon_s \left(1 + e\right) g_0\right]^2. \tag{11}$$

The solid's bulk viscosity is obtained from Lun *et al.*[28]

$$\lambda_s = \frac{4}{3} \varepsilon_s \rho_s d_s g_0 \left(1 + e\right) \sqrt{\frac{\Theta}{\pi}}. \tag{12}$$

There are two important parameters of kinetic theory of granular flow: the radial distribution function g_0 and the particle collision restitution coefficient e. The radial distribution function is a measure for the probability of interparticle contact and the model used here was proposed by Ding and Gidaspow.[21] Since there exists a thin liquid film covering the particle surface the restitution coefficient is always set to 1.0 in the sedimentation simulations.

3. Numerical method

The above governing equations for multiphase flows are fully coupled and an efficient solution depends on the type of algorithm to be used. Current multiphase CFD codes treat the interphase coupling terms semi-implicitly using two methods: SIMPLE-PEA or PC-SIMPLE. The SIMPLE-PEA is an extension of the SIMPLE scheme of Patankar[29] and was introduced by Spalding.[30] PEA stands for Partial Elimination Algorithm in which static pressure correction is executed with a mass balance of the gas phase and a similar solid pressure correction with that of the solid phase. Instead of respective pressure corrections for the two phases the PC-SIMPLE algorithm uses a shared pressure-correction equation for both phases based on total volume fraction conservation and the coupling between phases is accomplished implicitly at the level of the solution matrix using a block algebraic multigrid solver. The PC-SIMPLE algorithm has been implemented into the commercial CFD software Fluent version 6.1 (Fluent Inc., USA) and the governing equations of Eulerian two-fluid model are discretized based on unstructured mesh using a finite volume method. More details can be found on Fluent online document and in the work of Vasquez and Ivanov.[31] All the simulations in this work were carried out using Fluent 6.1 with a second-order upwind scheme for the convective terms.

4. Numerical results and discussions

4.1. Simulation of vertical bimodal sedimentation

First we simulated the bimodal suspension sedimentation of glass beads in the experiment of Davis *et al.*[32] The sedimentation column in the experiment was vertical, 100cm tall and has a square cross-section with 5cm each side. Two kinds of glass beads were used with the small bead mean diameter 137μm and the larger 198μm. To deal with the two kinds of particles we used a multi-group model where

two sets of particle equations are involved and the particle-particle drag coefficient is modelled according to Syamlal.[33] It should mentioned that the implicit coupled solution of multiphase Eulerian equations is very time consuming to achieve a high precision, so all simulations in our numerical test are carried out in a two- dimensional domain. The numerical parameters of bimodal sedimentation are specified in Table 1.

Table 1. Parameters of bimodal sedimentation simulation.

Group 1 particle diameter, density	137μm, 2440kg/m^3
Group 2 particle diameter, density	198μm, 2990kg/m^3
Group 1 initial particle volume fraction	0.03
Group 2 initial particle volume fraction	0.01
Fluid viscosity, density	0.0677 kg/(m·s), 992kg/m^3
x-domain	5cm
y-domain	100 cm
Number x-cells	16(uniform)
Number y-cells	160
Boundary conditions for fluid phase	No-slip at four sides
Boundary conditions for particle phase	Slip
Maxim particle volume fraction	0.53

Figure 1 shows the calculated transient levels of the two suspension interfaces compared with experimental data. The results of the Eulerian multiphase model agree very well with experiment. Several regions can be observed from the particle volume fraction contours in Fig.2. The top region is fluid, the next region is light particles and fluid, and the lower region contains fluid, light particles and heavy particles, just as discussed by Snider *et al*[13] that each region above the previous region contains one less species. From the drag coefficient formula we can clearly see that small particles have a higher interphase drag force that causes a lower sedimentation velocity than larger particles, which is just the separation mechanism of polydisperse suspension mixture.

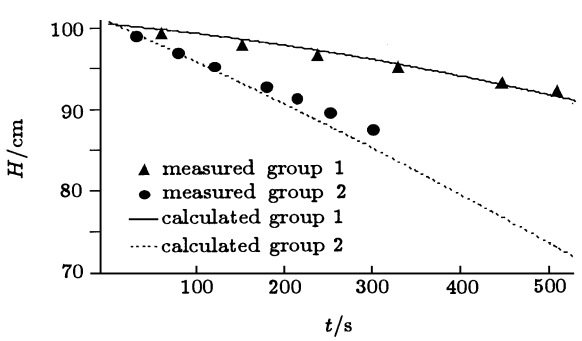


Fig.1. Sedimentation levels of bimodal suspension.

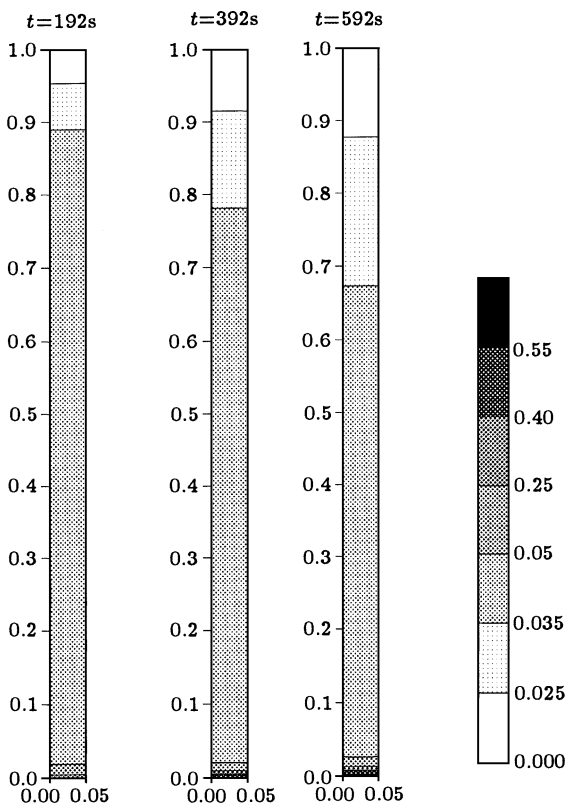


Fig.2. Particle volume fraction for bimodal suspension sedimentation.

4.2. Simulation of inclined sedimentation

Three numerical experiments were performed to study the physical process of sedimentation in vessels having different inclination angles (α=0°, 20°, 35°).

We used a hybrid mesh system for inclined sedimentation in which non-uniform quadrilateral grids combine with paved triangular grids as showed in Fig.3(a). The fluid property is the same as the bimodal sedimentation simulation and the particle mean diameter is 137μm. The initial particle volume fraction is 0.1 and the initial suspension interface height is H_0=40cm.

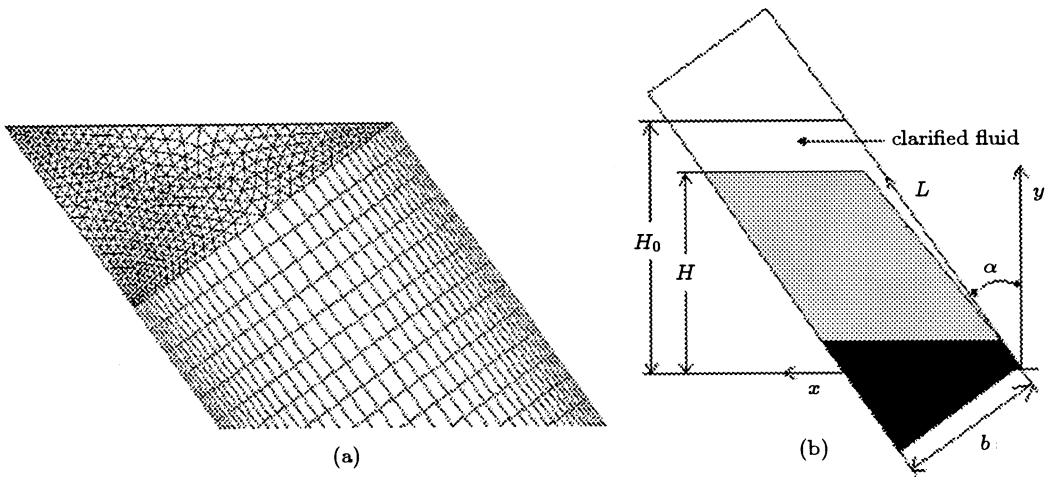


Fig.3. (a) The numerical mesh system for inclined containers (part of domain). (b) Illustration of inclined sedimentation.

Figure 4 shows the calculated interface levels compared with experiments and Fig.5 shows contours of particle volume fraction as well as fluid velocity vectors for different inclination angles at 300s. The Eulerian model captures the circulating flow patterns and the vortex centre moves downward within the suspension region. The flow patterns in this region are very similar to natural convection past a heated surface. Figure 6 gives fluid velocity vectors at different time for container tilted 20°.

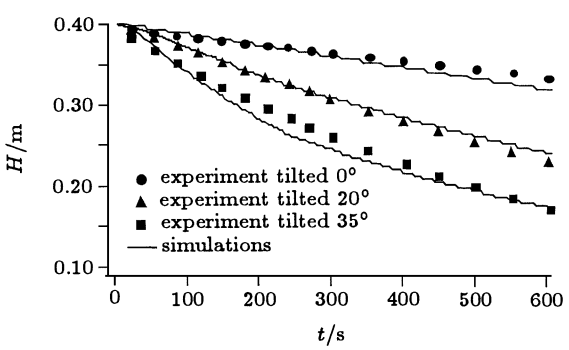


Fig.4. Simulated and measured interface of particle suspension at different angles.

In the clear fluid region there exists a very thin clarified fluid layer near the downward facing wall observed in experiments with the measured width of 0.1–0.25cm. Acrivos[9] determined that the thickness of this particle-free layer is given approximately by

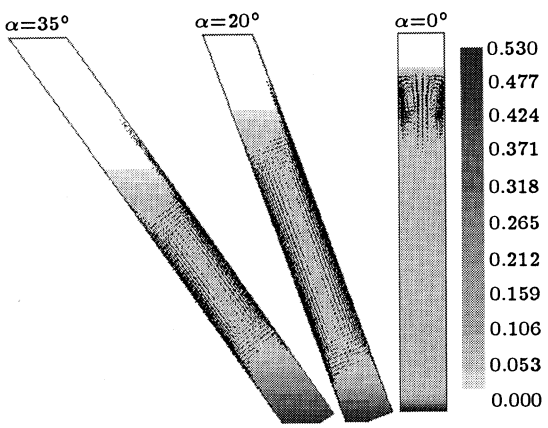


Fig.5. Particle volume fraction overlapped with fluid velocity vector at t=300s.

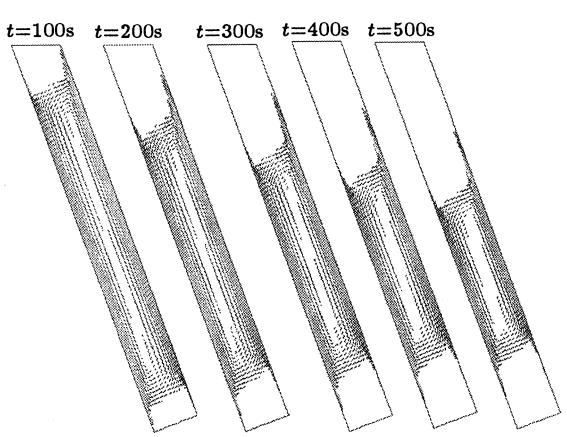


Fig.6. Velocity vectors at different time showing the circulating flow pattern.

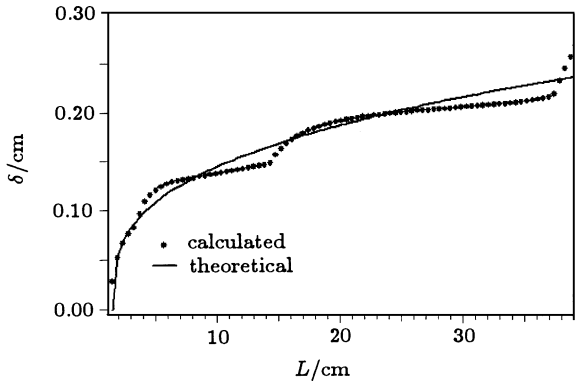


Fig.7. Calculated width of clear-fluid layer versus the distance along the downward-facing surface compared with theoretical predictions.

$$\delta = \left(3x\Lambda^{-1}\tan\alpha\right)^{1/3}, \qquad (13)$$

where Λ is the ratio of Grashoff number to particle Reynolds number. To resolve this thin layer we used the non-uniform grid that is very fine near the downward and upward facing walls just as Fig.3(a) shows. Figure 7 shows the calculated clear-fluid width compared with theoretical predictions for inclined sedimentation ($\alpha = 35°$) at time t=100s. They agree very well. Herbolzheimer[10] observed wave formations at the interface between this clarified thin layer and the particle suspension layer. The instabilities occurred for the vessel at small angles of inclination and were not present at large angles and the wave amplitude is comparable to the thickness of the clear fluid layer. In Fig.7 the jumping thickness at L=15 cm is about 0.1cm which compares reasonably with observations.

In our simulations the boundary conditions for particle phase are all set as slip boundaries which are different from the gas-particle system in which a no-slip or partial-slip wall boundary condition was proposed by Gidaspow.[22] In a liquid-particle system the particle's surface has a thin liquid film to lubricate the particle movement at walls. We did use no-slip boundary conditions in test simulations but little difference was seen for the prediction of sedimentation rate. The boundary conditions of fluid phase were set as no-slip boundaries except for the top wall. In the experiments there exists a free surface so we used a slip boundary condition for the fluid phase at the top wall. This conforms better to real experiments than using a no-slip boundary condition.

4.3. Circulating flows in vertical sedimentation

Figure 5 shows that there exist two vortices of sedimentation flows in the vertical container, which is different from the flow structure of inclined sedimentation flows. To investigate this phenomenon and understand what affects the flow structure, three sensitivity simulations are carried out. Three parameters, namely the fluid viscosity, container side's boundary conditions and container aspect ratio are selected for sensitivity tests and configurations for the base case and the sensitivity cases are listed in Table 2.

Table 2. Parameters for vertical sedimentation simulations.

Base case	
Fluid viscosity	0.001kg/(m·s)
Fluid density	998kg/m^3
x-domain	5cm
y-domain	40cm
Particle density	2420kg/m^3
Particle diameter	137μm
Boundary conditions for particles	Slip
Boundary conditions for fluid	No-slip
Initial volume fraction of particle	0.1
Number x-cells	36(non-uniform)
Number y-cells	100
Case 1	
Fluid viscosity	0.0677kg/(m·s)
Case 2	
Boundary conditions for fluid	Slip at left and right walls
Case 3	
x-domain	40cm
y-domain	40 cm
Number x-cells	50(non-uniform)
Number y-cells	50

Figure 8 shows the particle volume fraction and fluid stream function contours at different time for the base case. The two vortices are always in the particle suspension region near the left and right wall, respectively. A larger viscosity of fluid changes the vortex shape and the dual-circulation flow structure develops more slowly as Fig.9 shows (case 1). The distance between two vortices is much shorter because the velocity boundary layer of larger viscosity fluid in case 1 is much thicker than that of base case. Incidentally, the two vortices are almost symmetric.

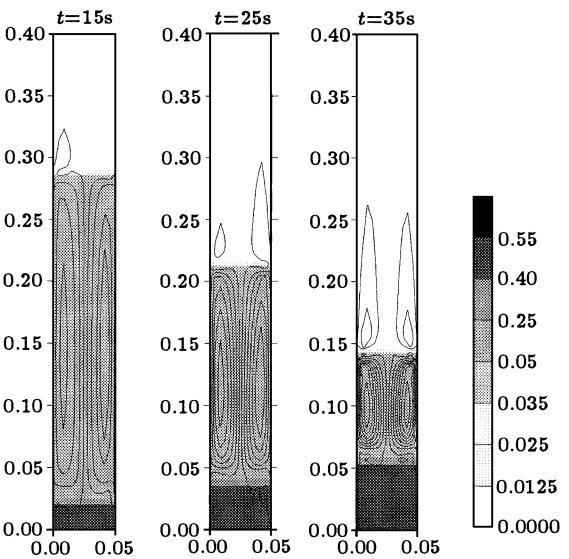


Fig.8. Particle volume fraction and fluid stream function of base case simulation.

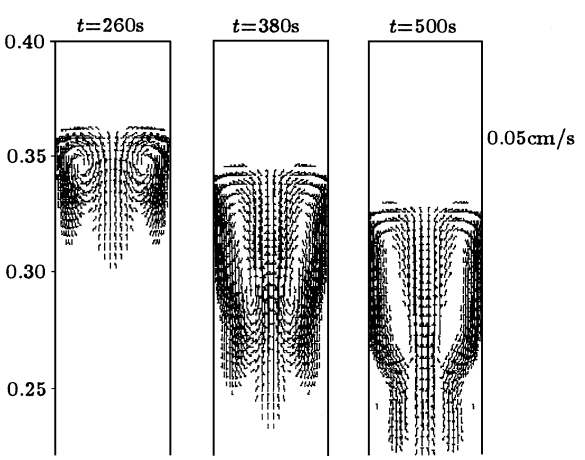


Fig.9. Fluid velocity vector at different time of case 1.

If the left and right walls of the container are set as slip boundary to fluid phase as in case 2, the circulating flow patterns will not occur (Fig.10(b)). The fluid flow seems to be homogeneous and no reversion (with a negative value) of vertical velocity occurs until the packed state of the particle phase. In case 3 the aspect ratio of container was set to 1:1 with width 0.4m and height 0.4m. The near wall dual vortices still can be seen in our simulation (Fig.10(a)). Obviously the boundary layer effect of the viscosity wall is the key to induce this phenomenon.

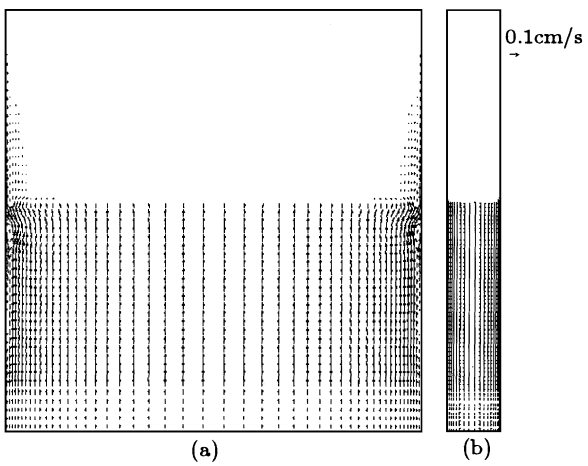


Fig.10. Fluid velocity vector of (a) case 3 and (b) case 2 at t=25s.

Figure 11 shows the profile of fluid vertical velocity at a typical height where the two vortices are located. Except for case 2, the vertical velocity reversion of fluid phase indicates the dual-vortex flow structure.

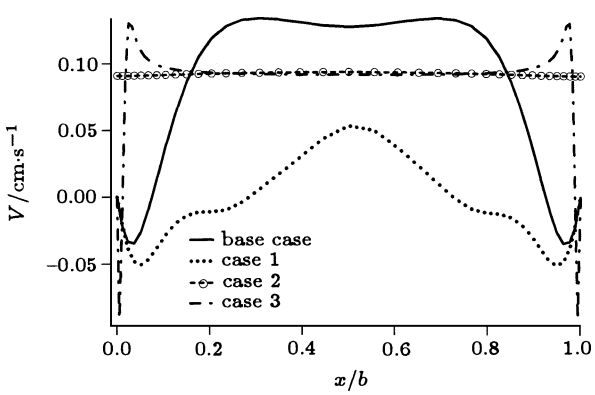


Fig.11. Fluid vertical velocity profile at a typical height.

We can analyse the boundary effect from the whole sedimentation process. At the beginning of batch sedimentation the particles accelerate downward due to the dominating gravity force and the fluid flows upward due to the incompressible continuity requirement. The fluid phase velocity is zero at the wall, thus in the developing boundary layer the fluid velocity is much smaller than the mean up-flow velocity. In contrast, the particle phase velocity is much larger

at the boundary layer than the mean sedimentation velocity because of a smaller drag force from the fluid phase. The inhomogeneous characteristic of particle sedimentation velocity results in a transient horizontal gradient of particle volume fraction at the interface between suspension and clarified fluid and thus forms the solids pressure gradient. Only the two-phase drag force in this direction can balance this pressure gradient at the interface:

$$-C\frac{\partial \varepsilon_{\mathrm{s}}}{\partial x} + \beta(u_{\mathrm{c}} - u_{\mathrm{s}}) = 0.$$

The solid pressure gradient drives the particles to move towards the lateral walls and at the same time the fluid is carried to lateral walls by the particle drag force. This flow tendency accelerates the particle to settle down near the walls and finally drives the fluid to circulate symmetrically near each lateral wall in the suspension region.

5. Conclusion

Sedimentations of dense particles in vertical and inclined vessels are simulated using an Eulerian two-fluid model and the viscosity and collision stress of particulate phase are modelled by the kinetic theory of granular flows. The multi-group particle model is used to solve the polydisperse sedimentation flows. The calculated sedimentation rates for both the vertical, inclined and bimodal solution mixtures compare well with experimental data. The clarified layer in inclined walls was predicted at the upper wall and its width agrees very well with theoretical analysis.

There exists a very rapid circulation in the particulate flow of inclined sedimentation but a dual-circulation flow structure is found in that of vertical sedimentation. Several sensitivity tests are simulated which predict that a smaller viscosity of the fluid phase makes the near-wall vortices slimmer and the boundary layer effect at the no-slip lateral walls are the main factor to induce the dual-vortex flow pattern in vertical sedimentations.

References

[1] Boycott A E 1920 *Nature* **104** 532

[2] Richardson J F and Zaki W N 1954 *Transactions of the Institution of Chemical Engineers* **23** 35

[3] Batchelor G K 1972 *J. Fluid Mech.* **52** 245

[4] De Kruif C G, Jansen J W and Vrij A 1987 *Physics of Complex and Supramolecular Fluids* (New York: Wiley Interscience) 315

[5] Ponder E 1925 *Q. J. Exp. Physiol.* **15** 235

[6] Nakamura H and Kuroda K 1937 *Keijo J. Med.* **8** 256

[7] Kinosita K 1949 *J. Colloid Interface Sci.* **4** 525

[8] Hill W D, Rothfus R R and Li K 1977 *Int. J. Multiphase Flow* **3** 561

[9] Acrivos A and Herbolzheimer E 1979 *J. Fluid Mech.* **92** 435

[10] Herbolzheimer E 1983 *Phys. Fluids* **26** 2043

[11] Zhou Z X and Lin J Z 1997 *Appl. Math. Mech.* **18** 543

[12] Lin J Z and Nie D M 2003 *Appl. Math. Mech.* **24** 631

[13] Andrews M J and O'Rourke P J 1996 *Int. J. Multiphase Flow* **22** 379

[14] Snider D M, O'Rourke P J and Andrews M J 1998 *Int. J. Multiphase Flow* **24** 1359

[15] Xu B H, Yu A B, Chew S J and Zulli J 2000 *Powder Technol.* **109** 13

[16] Longston P A, Al-Awamleh M A, Fraige F Y and Asmar B N 2004 *Chem. Eng. Sci.* **59** 425

[17] Goldschmidt M J V, Beetstra R and Kuipers J A M 2004 *Powder Technol.* **142** 24

[18] Patankar N A and Joseph D D 2001 *Int. J. Multiphase Flow* **27** 1685

[19] Fang H P and Chen S Y 2004 *Chin. Phys.* **13** 47

[20] Chen S, Shi B C, Liu Z H, He Z, Guo Z L and Zheng C G 2004 *Chin. Phys.* **13** 1657

[21] Ding J and Gidaspow D 1990 *AICHE J.* **36** 523

[22] Gidaspow D 1994 *Multiphase Flow and Fluidization–Continuum and Kinetic Theory Descriptions* (San Diego, CA: Academic)

[23] Syamlal M, Rogers W and O'Brien T J 1993 *MFIX Documentation: Volume 1 Theory Guide* (Springfield, VA: National Technical Information Service) Technical Report DOE/METC-9411004, NTIS/DE9400087

[24] Wu Y and Gidaspow D 2000 *Chem. Eng. Sci.* **55** 573

[25] Chapman S and Cowling T G 1979 *The Mathematical Theory of Non-Uniform Gases* (London: Cambridge University Press)

[26] Savage S B and Jeffrey D J 1981 *J. Fluid Mech.* **110** 255

[27] Jenkins J T and Savage S B 1983 *J. Fluid Mech.* **130** 187

[28] Lun C K K, Savage F B, Jeffrey D J and Chepurniy N 1984 *J. Fluid Mech.* **140** 223

[29] Patankar S V 1980 *Numerical Heat Transfer and Fluid Flow* (New York: Hemisphere)

[30] Spalding D B 1980 in *Recent Advances in Numerical Methods in Fluids* (Swansea: Pineridge Press) 139

[31] Vasquez S A and Ivanov V A 2000 *Proc. ASME FEDSM'00: ASME 2000 Fluids Engineering Division Summer Meeting* (Boston, MA) p743

[32] Davis R H, Herbolzheimer E and Acrivos A 1982 *Int. J. Multiphase Flow* **8** 571

[33] Syamlal M 1987 *The Particle–Particle Drag Term in a Multiparticle Model of Fluidization* (Springfield, VA: National Technical Information Service) Topical Report DOE/MC/21353-2373 NTIS/DE87006500